kν Correlation Analysis. A Quantitative Two-Dimensional IR Correlation Method for Analysis of Rate Processes with Exponential Functions

Saratchandra Shanmukh and Richard A. Dluhy*

Department of Chemistry, University of Georgia, Athens, Georgia 30602-2556

Received: January 21, 2004; In Final Form: April 30, 2004

A modified two-dimensional infrared correlation technique called *kν* correlation analysis is introduced. In this method, a mathematical asynchronous cross-correlation is performed between a set of *N* infrared spectra undergoing a dynamic intensity variation against a set of exponential functions that encompass a user-defined range of rate constants. The observed correlation intensities are a function of the rate constant of the exponential function and the spectral frequency. The *kν* correlation plots reveal the rate relationships between different molecular groups in terms of a quantitative and tangible parameter, *k*, which is the rate constant of the exponential function used in the correlation. A new parameter, the effective rate constant, k_{eff}, is defined as the point of maximum correlation intensity at particular frequencies in the plot of *k* vs *ν*. The calculated values of k_{eff} represent the relative rates at which the intensities of the spectral bands change during the course of the dynamic experiment. As a result, these k_{eff} values are comparable and can be used to assign quantitative rate relationships. By using simulated IR spectra, it was shown that the k_{eff} parameter is sensitive to the relative order in which the intensity change occurs, while the size of the correlation peaks gives an indication of the magnitude of the intensity change. Spectral bands whose rate of intensity change varies through a dynamic data set are distinguished by the presence of both positive and negative peaks in the *kν* correlation plots. We applied the *kν* correlation analysis method to the time-dependent IR spectra of the photoinitiated polymerization reaction of ethyl 2-cyanoacrylate. Analysis of the k_{eff} effective rate constants showed that vibrational modes corresponding to the monomeric and polymeric cyanoacrylate molecules react differently depending on whether an inhibitor is present.

Introduction

Two-dimensional infrared correlation spectroscopy (2D IR) has proven to be a valuable tool due to its ability to enhance spectral resolution and identify overlapped spectral features.[1−3] Two-dimensional IR spectroscopy is based on the correlation of dynamic spectral variations induced by an external sample perturbation. The effect of these perturbation-induced changes in the local molecular environment is manifested as either time-depdendent or external physical variable-dependent changes in IR spectral parameters. These resulting dynamic spectra are subject to a cross-correlation analysis that produces two-dimensional maps that can enhance spectral information by spreading out the IR band intensities along two orthogonal axes. Two-dimensional spectroscopy has particular advantages in simplifying complex spectra, identifying inter- and intramolecular interactions, and facilitating band assignments.[4]

Literature references to 2D IR correlation analysis have predominately been in the area of polymer structure, an application for which the method was first developed.[5] However, the past few years have seen increasing application of this methodology to other scientific areas, including biochemistry[6−8] and surface monomolecular films.[9−12] Studies using 2D heterospectral correlations have appeared that enable comparisons to be made among a number of spectral techniques.[13,14]

Standard 2D IR methods have been most successfully employed in simplifying complex spectra and facilitating band assignments through resolution enhancement.[4] In addition to these uses, 2D IR can also be used to determine the temporal order of events that occur in a set of dynamically varying spectra upon sample perturbation. The basis for this determination is the relative signs of the synchronous and asynchronous cross-peak at coordinate (ν_1, ν_2) in the 2D correlation plots.[2]

Although standard 2D IR methods may be used to determine the relative sequence of molecular events, this procedure tends to be difficult to implement for highly overlapped spectra and may lead to uncertainties while comparing the signs of the numerous cross-peaks in the synchronous and asynchronous correlation plots. To more quantitatively describe the degree of coherence between spectral intensity changes and the sequence of molecular events in a set of dynamic spectra, we previously developed a new approach that utilizes defined mathematical models as complementary functions to experimental data sets in the correlation algorithm.[15] This approach makes use of the fact that infrared intensity variations can take the shape of, or can be approximated by, common mathematical functions. By correlating such functional forms against experimental spectra, it is possible to obtain quantitative information about phase relationships. The first method developed under this approach was *βν* correlation analysis, which makes use of sinusoidal curves that vary in their phase angles.[15] An asynchronous correlation was performed between the sinusoidal curves and the experimental data set and a new parameter called the effective phase angle, β_e, was used to describe the relative relationship between the signal variations. Bands with larger β_e values were shown to undergo changes earlier than bands with smaller β_e values. We have applied *βν* correlation analysis to changes in the IR spectra of surface monolayers and showed

* To whom correspondence should be addressed. Phone: (706) 542-1950. Fax: (706) 542-9454. E-mail: dluhy@chem.uga.edu.

10.1021/jp049689a CCC: $27.50
Published on Web 06/08/2004

how the relative rates of acyl chain and methyl group reorientation could be quantitatively determined,[11] and have also applied this method in probing the conformational states and relative reorientation rates of proteins at surfaces.[12]

In the current article we report on a new model-based approach to 2D correlation analysis that substitutes a different mathematical function for the sine function used in the $\beta\nu$ method. The selection of a particular model correlation function is dictated by the similarity of the function waveform with common infrared intensity variation profiles that are applicable to molecular systems; in the present case this is an exponential function. A new model-based 2D correlation method called *kν correlation analysis* is introduced in which a set of dynamic spectra are correlated against a set of exponential curves that differ in their rate constants. As in the previously described $\beta\nu$ correlation method, *kν* correlation analysis employs an asynchronous cross correlation since this calculation is more sensitive to intensity changes and spectral resolution enhancement than is the synchronous correlation. A quantitative parameter, the *effective rate constant*, k_{eff}, is defined and used to establish relative rate relationships between spectral intensity variations. Different intensity variation models composed of simulated spectra are used to illustrate the ability of the *kν* correlation method in distinguishing between processes occurring with different rates of change. This method, as well as the previously described $\beta\nu$ correlation method, is applicable not only to IR spectroscopy, but also to spectra obtained from such methods as fluorescence, Raman, and near-infrared spectroscopy to obtain information about relative rates in a set of dynamically varying spectra. To demonstrate the utility of the *kν* method, we studied the anionic polymerization of cyanoacrylate using the classic metallocene ruthenocene as a photoinitiator. This reaction was monitored with ATR-IR spectroscopy and *kν* correlation analysis was applied to the time-dependent spectra to elucidate the rates of intensity change in the different vibrational modes attributable to the monomeric and the polymeric cyanoacrylate species.

Materials and Methods

Reagents. Ruthenocene ($RuCp_2$; CP_2 is η^5-C_5H_5) was obtained from Sigma-Aldrich (St. Louis, MO) at 97% purity and was further purified by vacuum sublimation. High-purity ethyl 2-cyanoacrylate (CA) was obtained from Loctite Corp. (Rocky Hill, CT) at 99.9% purity and was used as received; the colorless liquid monomer contained trace amounts of hydroquinone and methane sulfonic acid as scavengers for adventitious radical and basic impurities, respectively. Tetrahydrofuran (THF) was obtained from Fisher Scientific (Fairlawn, NJ) and used without further purification.

IR Spectroscopy. Attenuated total reflectance infrared (ATR-IR) spectra were acquired with a BioRad/Digilab (Cambridge, MA) FTS-60 FT-IR spectrometer equipped with a LN_2-cooled, narrow-band HgCdTe detector. Kinetic IR studies of the rate of photoinitiated polymerization of ethyl 2-cyanoacrylate were conducted on freshly prepared solutions of CA containing the ruthenocene photoinitiator. A solution of CA in THF (2:3 (v:v)) was prepared to which $RuCp_2$ was added at a concentration of 12 mM. A small volume (~0.3 mL) of this sample solution was placed on a germanium ATR crystal mounted in a horizontal ATR accessory (CIC Photonics, Albuquerque, NM) within the sample chamber of the spectrometer. Polymerization of the CA sample commenced upon irradiating the sample with the polychromatic output of a mercury-arc lamp at 110 mW. Incident light intensity at the sample was measured with a Coherent (Santa Clara, CA) Model 10 power meter. ATR-IR spectra were collected every 1.5 s with use of the following parameters: one co-added scan, triangular apodization with one level of zero-filling, and 4-cm^{-1} resolution. Spectra were analyzed with the GRAMS 32/AI spectra software package (Ver. 6.0, Galactic Industries, Salem, NH).

Calculation of 2D IR Correlation Spectra. The 2D IR synchronous spectrum, $\Phi(\nu_1,\nu_2)$, and the asynchronous spectrum, $\Psi(\nu_1,\nu_2)$, were calculated as previously described.[11,12,15] These algorithms use the most recent mathematical formulation in which a Hilbert transform is utilized for calculating the asynchronous spectrum rather than the more commonly employed Fourier transform.[16] In all cases the average spectrum was subtracted from each time-dependent, sequentially obtained ATR-IR spectrum to produce a set of dynamic IR spectra. The resulting dynamic spectra were then used in the correlation analysis. Before 2D correlation analysis, the dynamic spectra were baseline corrected with the GRAMS/AI spectral software package.

The asynchronous 2D plots presented in this article were calculated by using 2D IR correlation analysis algorithms written in our laboratory, using the MATLAB programming environment (Version 6, The MathWorks, Inc., Natick, MA).

Simulated Spectra. Computer-generated simulated IR spectra were calculated with an Array Basic program written in our laboratory for the Grams/AI environment (R. Dluhy, unpublished). All synthetic spectra were calculated by using Lorentzian band shapes with a resolution of 1.0 cm^{-1}. Full widths at half-maximal peak intensity for the simulated band shapes were 10.0 cm^{-1}. No additional noise was added to the simulated spectra.

Results and Discussion

I. *kν* Correlation Analysis: A Modified 2D IR Method for Calculating Exponential Correlations. In previous work, we introduced a modified two-dimensional infrared correlation method, called $\beta\nu$ correlation analysis, for quantitatively determining the relative rates of intensity change and the degree of coherence between intensity variations in a discrete set of dynamic spectra.[15] In this method, a mathematical cross correlation is performed between a set of spectra undergoing some dynamic variation against a simple mathematical function, which we chose to be a sine function. In $\beta\nu$ correlation analysis, the calculated correlation intensities are a function of the phase angle (β) of the sinusoidal function and the spectral frequency (ν). The maximum positive correlation intensity will be observed at one point in the (β,ν) correlation plot. This point is used to define a new parameter, the effective phase angle, β_e, of $f(\nu,n)$, where, for the range $360° \geq \beta \geq 0°$, β_e is simply equal to $\beta + 90°$. We have applied classical 2D IR as well as $\beta\nu$ correlation spectroscopy to several model systems, including the in situ IR spectroscopy of monomolecular films.[11,12] The $\beta\nu$ method enabled us to identify specific molecular conformations and to follow the reorientation of these molecular groups as a function of an external perturbation.

Other researchers have also explored the utility of model-dependent correlation methods for processing nonperiodic perturbations. For example, Eads and Noda applied generalized correlation analysis for processing two-dimensional arrays of NMR spectra.[17] This work used both the cross-correlation between experimental spectra as well as model-based correlation analyses to obtain quantitative diffusion coefficients. The data set used for the model-based analysis was comprised of a set of Gaussian curves generated with logarithmically spaced diffusion coefficients.

In our current work, we have expanded the scope of our previous model-dependent correlation method by replacing the

mathematical function used in the correlation analysis. The selection of a particular model correlation function is dictated by the similarity of the function waveform with common infrared intensity variation profiles that are applicable to molecular systems; many different functional forms are potential candidates. The new method assumes an exponential relationship between spectral intensities in the dynamic data set. In this updated approach, a mathematical asynchronous cross-correlation is performed between a set of N infrared spectra undergoing a dynamic intensity variation against a set of exponential functions that encompass a range of rate constants. In keeping with the terminology introduced with the $\beta\nu$ method, we call this new method $k\nu$ correlation analysis, since the calculated correlation intensities are a function of the rate constant (k) of the exponential function and the spectral frequency (ν). The $k\nu$ two-dimensional correlation plots reveal rate relationships between different molecular events in terms of a quantitative and tangible parameter, k, which is the rate constant of the exponential function used in the correlation. As such, it is a model-dependent 2D IR correlation method analogous to the $\beta\nu$ correlation analysis described in our earlier papers.

An asychronous $k\nu$ correlation analysis is mathematically described in eq 1. The correlation intensity Ψ at some point (ν,k) represents the correlation of the measured IR spectral intensity $y(\nu,n_j)$ with the mathematical function $\exp(-kt + R)$. In eq 1, y is the spectral intensity; ν is the frequency or wavenumber; n_j is the number of the spectrum in the ordered sequence where the first spectrum number is zero; k is the rate constant of the exponential curve; N is the total number of spectra used in the calculation; R is a constant matrix; and M_{jk} is the Hilbert−Noda transform matrix[16] defined in eq 2.

$$\Psi(\nu,k) = \frac{1}{N-1}\sum_{j=0}^{N-1} y(\nu,n_j)\sum_{k=0}^{N-1} M_{jk}\exp(-kt + R) \qquad (1)$$

$$M_{jk} = \begin{cases} 0 & \text{if } j = k \\ 1/\pi(k-j) & \text{otherwise} \end{cases} \qquad (2)$$

The asynchronous $k\nu$ correlation intensity can be either positive or negative depending on the direction and magnitude of intensity change. Based on studies done on simulated spectra, which are described below, positive peaks are observed when the rate of intensity variation increases and negative peaks are observed when the rate of intensity variation decreases. In the cases of bands where the direction of intensity change alters during the course of the experiment, or when the rate of intensity change varies, both positive and negative correlation peaks may be observed for a single spectral band.

A new parameter, the *effective rate constant*, k_{eff}, is defined from the $k\nu$ correlation plot. This k_{eff} parameter is defined as the point of maximum correlation intensity in the plot of k vs ν. The range of values that k_{eff} can take may be arbitrarily set and is between 1 and 7 in the current work. The calculated values of k_{eff} are representative of the rates at which the intensities of the spectral bands change during the course of the dynamic experiment. These k_{eff} values are not the actual kinetic rate constants per se, but are instead the *relative differences* of the rates defined by the rate constants used in the 2D correlation calculation. As a result, these k_{eff} values are comparable and can be used to assign quantitative rate relationships. Events at frequencies with a larger k_{eff} value occur earlier than events at frequencies with smaller k_{eff} values. Positive and negative k_{eff} values are comparable and hence no manipulation of the spectra or the correlation plots is required to compare increasing and decreasing bands.

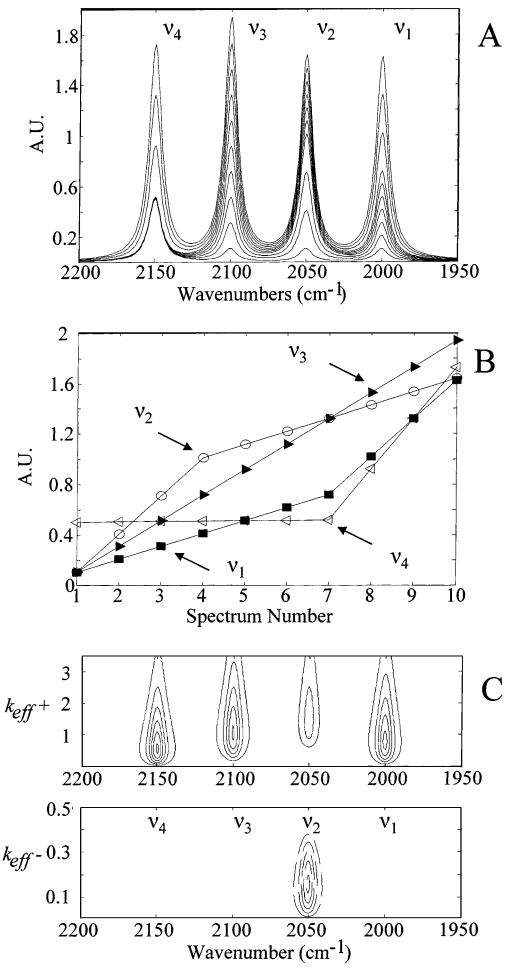

Figure 1. Simulated spectral model "A" with multistep linear intensity changes. (A) Simulated infrared spectrum with bands at $\nu_1 = 2000$ cm^{-1}, $\nu_2 = 2050$ cm^{-1}, $\nu_3 = 2100$ cm^{-1}, and $\nu_4 = 2150$ cm^{-1}. (B) Spectral intensity profile for the spectral bands. (C) $k\nu$ correlation plot of the above model.

The $k\nu$ plots of effective rate constants vs wavenumber were calculated by using $k\nu$ correlation analysis algorithms written in our laboratory using the MATLAB programming environment. As is the case with the traditional 2D IR correlation plots, the spectra used in the $k\nu$ plots were baseline corrected before calculation by using the GRAMS/AI spectral software package.

II. Simulated Spectral Models Used To Illustrate the *kν* Method. In this section we explore how specific mathematical forms of spectral intensity variation affect the calculated k_{eff} values. Within each model, we describe several different possible paths of intensity variation for an absorption band in a set of dynamic spectra. Each model system can then be used to explore how the calculated k_{eff} values respond to the specific forms of intensity variation. In doing this, we can establish a relationship between the calculated k_{eff} values and the relative rates of intensity change for the time-resolved absorption bands in a dynamic data set.

Model A. The first model that we consider for the application of the exponential correlation method consists of four spectral bands that exhibit linear increases in intensity through the data set (Figure 1A). In Model A, three of the four spectral bands increase in intensity, but in a two-stage increment in which there is a delay in the response of the individual features to the external perturbation. Figure 1B illustrates the variation of the band intensity for the four peaks in Model A through the data set. From the intensity changes seen in Figure 1B, the sequence

TABLE 1: Values of the Effective Rate Constants k_{eff}^{+} and k_{eff}^{-}, Obtained from the *kν* Correlation Plot in Figure 1[a]

band assign	wavenumber (cm^{-1})	k_{eff}^{+}	k_{eff}^{-}
ν_1	2000	0.35	–
ν_2	2050	0.82	0.13
ν_3	2100	0.50	–
ν_4	2150	0.27	–

[a] These effective rate constants were obtained from the simulated IR spectra in model A that represents a two-step linear intensity change.

of spectral events can be summarized as $\nu_2 \rightarrow \nu_3 \rightarrow \nu_1 \rightarrow \nu_4$ where "→" means "occurs before". A set of dynamic spectra was generated from the spectra in Figure 1A by subtracting the reference (average) spectrum from each individual spectrum. When calculating *kν* correlations for synthetic spectra, we used the average spectrum in the dynamic data set as the reference spectrum. Both the average spectrum and the zero spectrum were tried as references; however, the average spectrum was found to give more accurate results with these intensity models.

An asynchronous *kν* correlation was performed between the dynamic spectra generated from Figure 1A and a set of exponential curves that differed in their rate constants. The resulting *kν* correlation plot is shown in Figure 1C. In this plot, each of the four simulated peaks contain positive k_{eff} values, which is expected since all the spectral intensities increase during the course of the data set. The k_{eff} values corresponding to the four spectral bands are shown in Table 1 and can be used to determine the relative rates of intensity change in the four peaks in the model described previously. The k_{eff}^{+} values $0.82 > 0.5 > 0.35 > 0.27$ indicate the order of change in spectral intensities to be $\nu_2 \rightarrow \nu_3 \rightarrow \nu_1 \rightarrow \nu_4$, as was defined in the model. This result clearly demonstrates that k_{eff} values can be used to establish the relative rates of change in the band intensities of a set of time-resolved spectra whose intensities change in a defined fashion.

Figure 1C also shows that the ν_2 band at 2050 cm^{-1} has a negative k_{eff} value ($k_{eff}^{-} = 0.13$) associated with it. The negative peak in the *kν* plot is explained by the nature of the intensity variation for this band. As seen in Figure 1B, the 2050-cm^{-1} band intensity varies as a two-stage linear function: initially with a large positive slope, and then with a smaller positive slope (i.e. the rate of change decreases). The *kν* correlation method calculates the decrease in the rate of intensity change as a negative k_{eff} value since the rate of change decreased relative to the initial rate. The presence of a negative correlation peak for the 2050-cm^{-1} band illustrates that the *kν* correlation method is sensitive to the *change* in the relative rates of the band intensities through the dynamic data set. This is an advantage of the *kν* method over the previously published *βν* correlation analysis method.

Model B. This model, illustrated in Figure 2A, contains four simulated bands in which the band intensities increase in a two-stage linear fashion. In this case, all band intensities increase linearly after an initial lag period that differs for each band. The model was constructed such that the intensity of the band at ν_1 at 2000 cm^{-1} begins to increase before the ν_2 band at 2050 cm^{-1} increases, followed by the intensity increases of ν_3 (2100 cm^{-1}) and ν_4 (2150 cm^{-1}). The sequence of spectral events in panels A and B in Figure 2 can be summarized as $\nu_1 \rightarrow \nu_2 \rightarrow \nu_3 \rightarrow \nu_4$. A *kν* correlation was performed on the dynamic spectra generated from the spectral set. The resulting plot is presented in Figure 2C and the corresponding k_{eff} values are listed in Table 2. Four positive peaks were generated in the

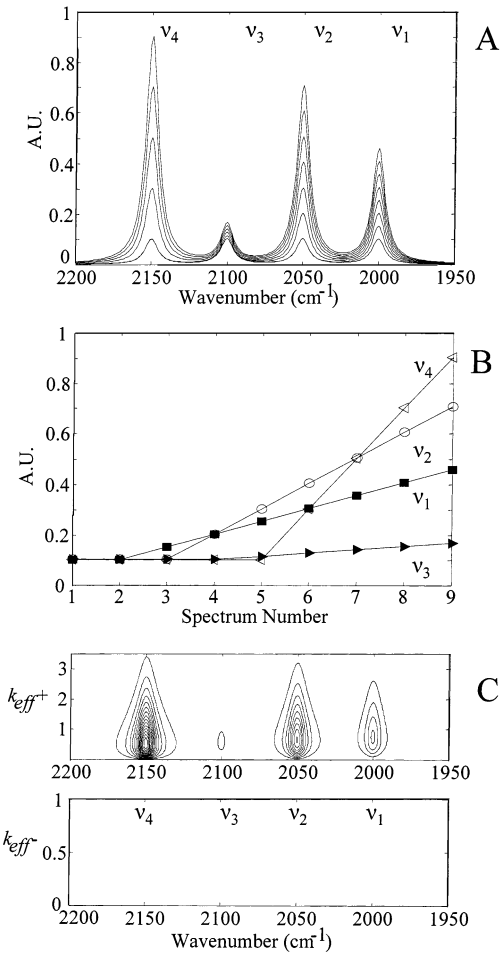

Figure 2. Simulated spectral model "B" with multistep linear intensity changes. (A) Simulated infrared spectrum with bands at $\nu_1 = 2000$ cm^{-1}, $\nu_2 = 2050$ cm^{-1}, $\nu_3 = 2100$ cm^{-1}, and $\nu_4 = 2150$ cm^{-1}. (B) Spectral intensity profile for the spectral bands. (C) *kν* correlation plot of the above model.

TABLE 2: Values of the Effective Rate Constants k_{eff}^{+} and k_{eff}^{-}, Obtained from the *kν* Correlation Plot in Figure 2[a]

band assign	wavenumber (cm^{-1})	k_{eff}^{+}	k_{eff}^{-}
ν_1	2000	0.45	–
ν_2	2050	0.39	–
ν_3	2100	0.35	–
ν_4	2150	0.30	–

[a] These effective rate constants were obtained from the simulated IR spectra in model B that represents a delayed linear intensity change.

corresponding *kν* plot shown in Figure 2C. From the k_{eff} values the following order of relative rates can be determined: ν_1 ($k_{eff}^{+} = 0.45$) → ν_2 ($k_{eff}^{+} = 0.39$) → ν_3 ($k_{eff}^{+} = 0.35$) → ν_4 ($k_{eff}^{+} = 0.30$). This corresponds to the order that was built into this intensity change model. This particular model indicates that the k_{eff} values are sensitive to the *order* in which the intensity change occurs, while the magnitude of the bands in the *kν* plot reflects the *degree* of the spectral intensity variation.

Model C. As seen in Figure 3A,B, this model consists of four spectral bands whose intensities increase exponentially with different rate constants. A *kν* correlation was performed on the dynamic spectra generated from the spectral set and the resulting correlation plot is presented in Figure 3C with the corresponding k_{eff} values listed in Table 3. The k_{eff} values for all four bands are positive since the bands are exponentially increasing in

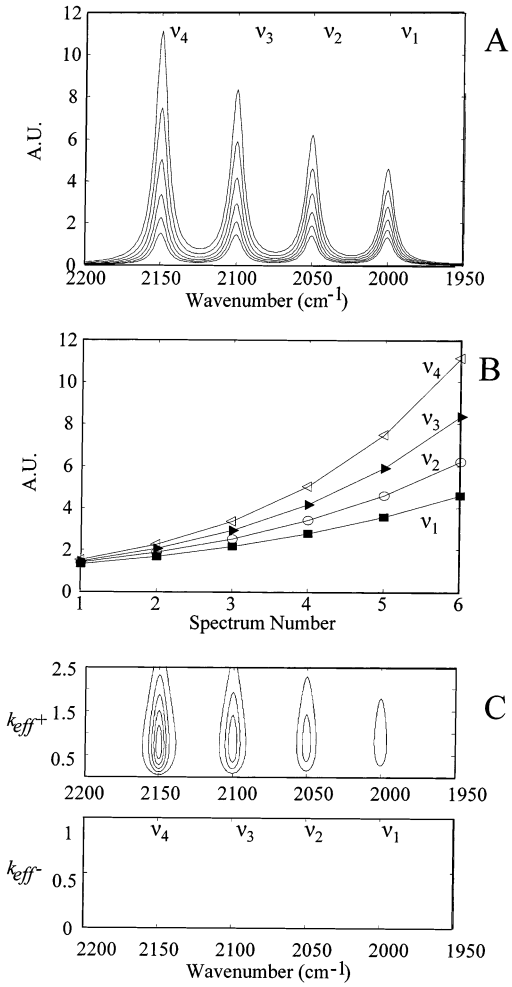

Figure 3. Simulated spectral model "C" with bands whose intensities increase exponentially. (A) Simulated infrared spectrum with bands at $\nu_1 = 2000$ cm^{-1}, $\nu_2 = 2050$ cm^{-1}, $\nu_3 = 2100$ cm^{-1}, and $\nu_4 = 2150$ cm^{-1}. (B) Spectral intensity profile for the spectral bands. (C) $k\nu$ correlation plot of the above model.

TABLE 3: Values of the Effective Rate Constants k_{eff}^{+} and k_{eff}^{-}, Obtained from the $k\nu$ Correlation Plot in Figure 3[a]

band assign	wavenumber (cm^{-1})	k_{eff}^{+}	k_{eff}^{-}
ν_1	2000	0.7	−
ν_2	2050	0.8	−
ν_3	2100	0.8	−
ν_4	2150	0.8	−

[a] These effective rate constants were obtained from the simulated IR spectra in model C that represents a delayed linear intensity change.

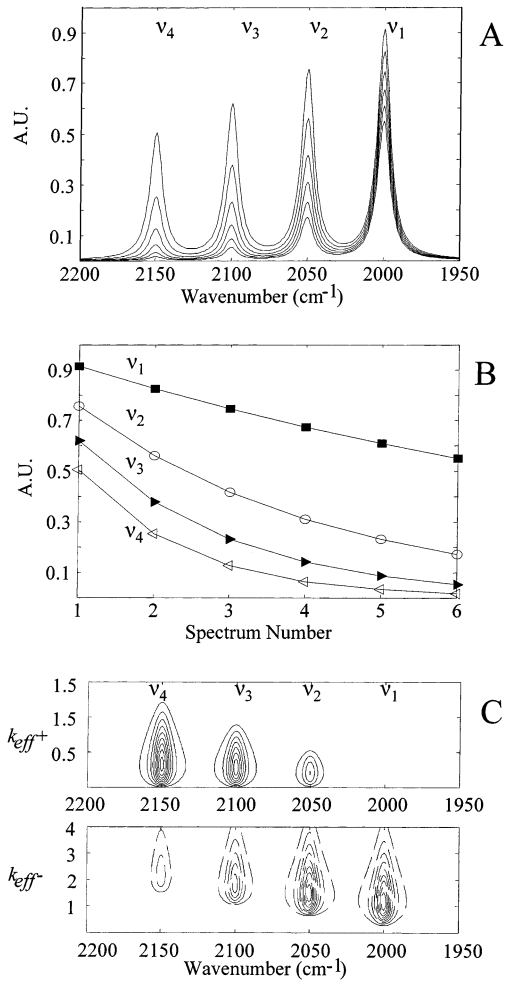

Figure 4. Simulated spectral model "D" with bands whose intensities decrease exponentially. (A) Simulated infrared spectrum with bands at $\nu_1 = 2000$ cm^{-1}, $\nu_2 = 2050$ cm^{-1}, $\nu_3 = 2100$ cm^{-1}, and $\nu_4 = 2150$ cm^{-1}. (B) Spectral intensity profile for the spectral bands. (C) $k\nu$ correlation plot of the above model.

TABLE 4: Values of the Effective Rate Constants k_{eff}^{+} and k_{eff}^{-}, Obtained from the $k\nu$ Correlation Plot in Figure 4[a]

band assign	wavenumber (cm^{-1})	k_{eff}^{+}	k_{eff}^{-}
ν_1	2000	−	1.1
ν_2	2050	0.2	1.4
ν_3	2100	0.2	1.8
ν_4	2150	0.3	2.2

[a] These effective rate constants were obtained from the simulated IR spectra in model D that represents a delayed linear intensity change.

intensity in the positive direction. In addition, all the bands in the simulated spectrum have approximately the same k_{eff}^{+} value of 0.8, which means that there is no asynchronicity between the rates of intensity change in these bands.

Model D. The final model in the analysis, shown in Figure 4A,B, consists of four simulated spectral bands whose intensities decrease exponentially with different rate constants. In terms of 2D correlation spectroscopy, an exponential decrease in band intensity can be understood as a delay in the response of the individual features to the external perturbation. A $k\nu$ correlation was performed between the dynamic data set calculated from the spectra in Figure 4A and a set of decreasing exponential curves that differed in their rate constants. The resulting $k\nu$ plot is presented in Figure 4C and the corresponding k_{eff} values for the observed peaks are listed in Table 4. As seen in Figure 4C, the $k\nu$ correlation plot for this model has negative peaks at all frequencies denoting a decrease in band intensity through the data set. However, the different k values calculated for each band denote the difference in the rate of decrease of the individual band intensities. From the negative k_{eff} values it can be seen that the ν_1 band at 2000 cm^{-1} ($k_{\mathrm{eff}}^{-} = 2.2$) has a higher rate of intensity change than do than the bands at ν_2 (2050 cm^{-1}, $k_{\mathrm{eff}}^{-} = 1.8$), ν_3 (2100 cm^{-1}, $k_{\mathrm{eff}}^{-} = 1.4$), and ν_4 (2150 cm^{-1}, $k_{\mathrm{eff}}^{-} = 1.1$). The different k_{eff}^{-} values represent the different rates at which the intensities of the respective bands change.

Figure 4C also shows that the bands at 2150, 2100, and 2050 cm^{-1} have a positive k_{eff} value associated with them: ν_4 (2150 cm^{-1}, $k_{\mathrm{eff}}^{+} = 0.30$), ν_3 (2100 cm^{-1}, $k_{\mathrm{eff}}^{+} = 0.20$), and ν_2 (2050

cm^{-1}, $k_{eff}^{+} = 0.20$). The positive peaks in the *kν* plot for this model are explained by the nature of the intensity decreases for these bands. The intensities for these three bands vary in a two-step process: initially with a large negative slope, and then with a smaller negative slope (i.e. the rate of decrease slows). The *kν* correlation method calculates the decrease in the rate of intensity change as a positive k_{eff} value since the rate of change increased relative to the initial rate. Similar to the case described above in Model A, the presence of positive and negative correlation peaks for an absorption band illustrates that the *kν* correlation method is sensitive to the *change* in the relative rates of the band intensities through the dynamic data set.

III. Application of the *kν* Method: Anionic Photopolymerization of Cyanoacrylate. Classical metallocenes such as ferrocene and ruthenocene ($FeCp_2$ and $RuCp_2$, where Cp_2 is η^5-C_5H_5) can be used as anionic photoinitiators for polymerization reactions. These metallocenes dissolve readily in a wide range of nonaqueous solvents, exhibit good thermal stability, and are photolytically inert in solution.[18] It has been shown that $FeCp_2$ and $RuCp_2$ form ground state donor−acceptor (D−A) complexes with electron-accepting solvents that are characterized by a charge-transfer-to-solvent (CTTS) absorption band in the near-UV region. Irradiation into this band causes the one-electron oxidation of the metallocenes to the corresponding metallocenium cation accompanied by reduction of the solvent to its radical anion.[19−22] Metallocene photooxidation also occurs in neat ethyl 2-cyanoacrylate (CA) to produce an initiating species for anionic polymerization.[23]

Photoinitiated polymerization of CA is characterized by an induction period followed by a rapid acceleration of the polymerization reaction that finally reaches a limiting value at ∼80−90% conversion. The induction period is attributed to the presence of methane sulfonic acid (MSA), which serves as a scavenger for adventitious traces of basic impurities in the commercial monomer. Polymerization is inhibited until sufficient anionic species are photochemically generated to neutralize this acid, whereupon rapid consumption of monomer commences. Not surprisingly, addition of extra MSA to a sample lengthens the induction period and slows the ensuing anionic polymerization.

We previously showed that the rate of photoinitiated polymerization in CA could be quantitative characterized by attenuated total reflectance infrared spectroscopy (ATR-IR).[23] This technique allows continuous monitoring of the polymerization occurring in a 2−3 μm layer of monomer immediately adjacent to the surface of the ATR crystal. In the current work we have taken the time-dependent ATR-IR spectra of the photoinitiated polymerization of CA and subjected them to generalized 2D IR as well as *kν* correlation analysis to elucidate the rate relationships between the different spectral features.

The ATR-IR spectra of the CA polymerization reaction are shown in Figure 5. Several vibrational modes are observed in the IR spectrum that are correlated with molecular changes occurring during polymerization,[24] for example: (1) The bands at 1190 and 1290 cm^{-1} are due to the stretching vibrations of the C−O bond of the ester that is conjugated to the C═C of the monomer. These two bands have approximately the same intensity and are characteristic of α,β-unsaturated esters. As the polymerization reaction proceeds and conjugation decreases, the infrared intensities of these bands decrease. (2) The band at 1250 cm^{-1} is due the C−O ester stretch of the polymeric cyanoacrylate molecule. This band increases in intensity during the polymerization process. (3) The band at 1616 cm^{-1} is due to the C═C stretch of the cyanoacrylate monomer molecule and decreases with time as the polymerization reaction proceeds. (4) The vibrational frequency of the C═O group increases from 1735 cm^{-1} for the conjugated ester to 1752 cm^{-1} for the saturated ester.

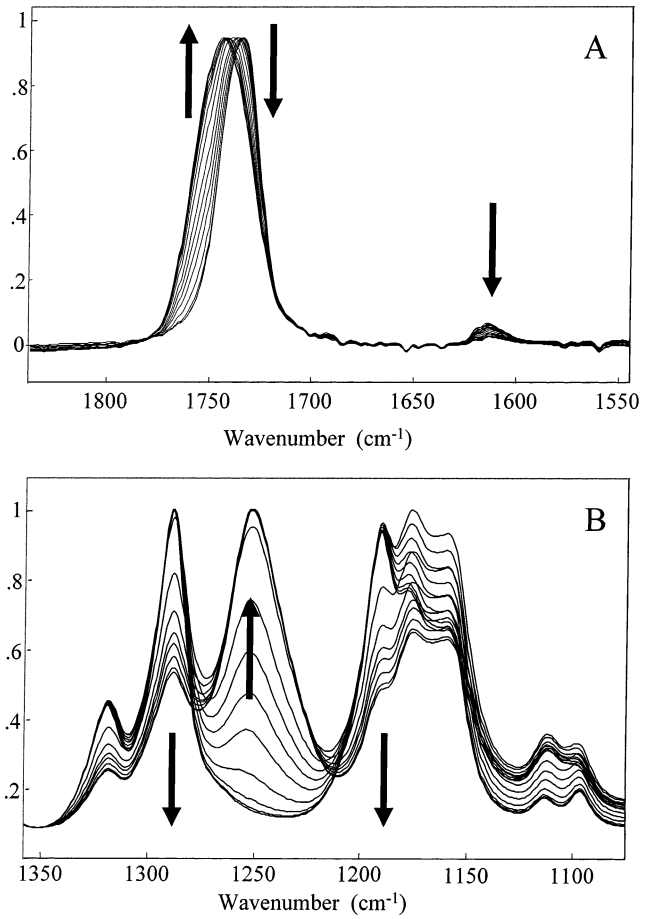

Figure 5. Time-dependent ATR-IR spectra of the ruthenocene-initiated polymerization reaction of cyanoacrylate collected over 300 s. Arrows designate the direction of increase or decrease in intensity for the indicated bands over the course of the polymerization reaction. (A) Spectral region showing the carbonyl (C═O) bands and the C═C band at 1616 cm^{-1}. (B) Spectral region showing the ester C−O bands due to the monomeric cyanoacrylate molecule at 1190 and 1290 cm^{-1} as well as the ester C−O band for the polymer at 1250 cm^{-1}.

Figure 6A illustrates the time-dependence of the intensity profiles of these vibrational modes for the case of the polymerization of CA in the absence of inhibitor, while Figure 6B illustrates the same data for the polymerization of CA in the presence of inhibitor. From Figure 6 the time regimes corresponding to maximal spectral intensity changes may be identified. We used the spectra between 20 and 42 s (16 spectra total) to characterize the polymerization reaction in the absence of inhibitor (Figure 6A) and the spectra between 94 and 191 s (65 spectra total) to characterize the reaction in the presence of inhibitor (Figure 6B).

The spectra in these time domains were analyzed by using conventional two-dimensional infrared correlation spectroscopy and *kν* correlation analysis to determine the relative rate relationships and degree of coherence among the molecular groups of CA during the photoinitiated polymerization process. The vibrational modes studied were 1190 (conjugated carbonyl ester C−O stretch), 1250 (saturated carbonyl ester C−O stretch), 1290 (conjugated carbonyl ester C−O stretch), 1616 (C═C stretch), 1732 (conjugated carbonyl ester C═O stretch), and 1753 cm^{-1} (saturated carbonyl ester C═O stretch).

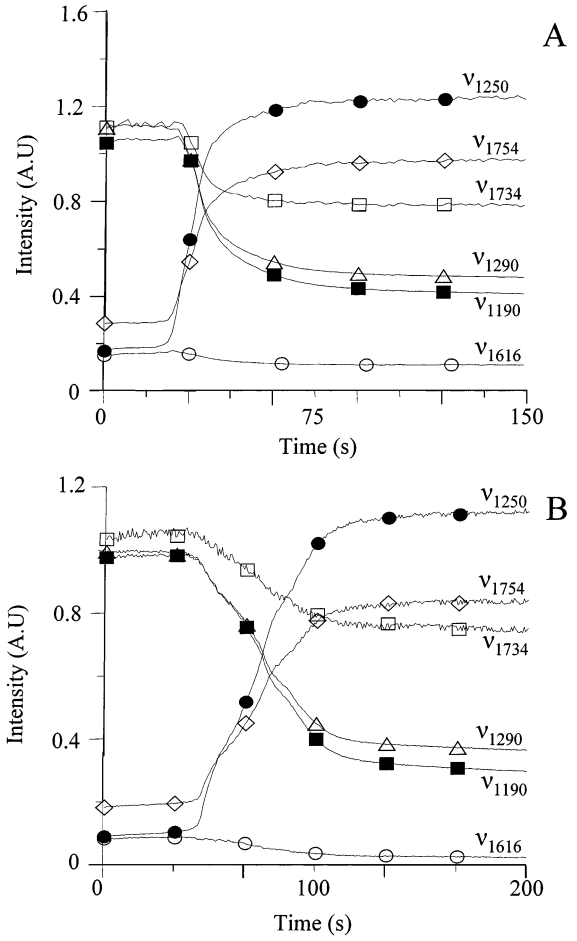

Figure 6. Spectral intensity profiles for the spectral bands shown in Figure 5 over the time course of the ruthenocene-initiated photopolymerization reaction of CA. The different bands shown are 1190 (■), 1250 (●), 1290 (△), 1616 (○), 1734 (□), and 1754 cm^{-1} (◇). (A) Intensity profiles for the CA bands during the polymerization reaction in the absence of an inhibitor. (B) Intensity profiles for the CA bands during the polymerization reaction in the presence of the inhibitor MSA.

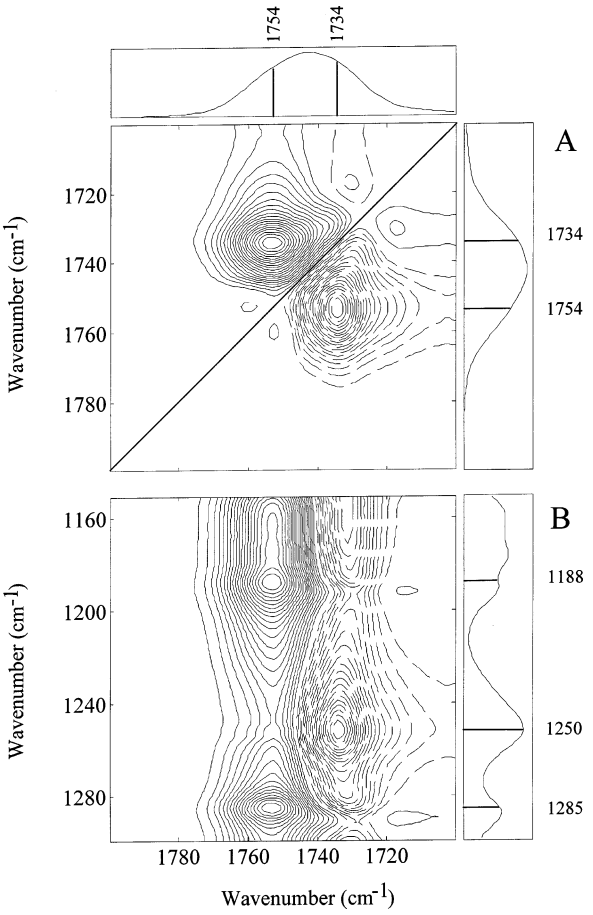

Figure 7. Asynchronous 2D IR correlation plots calculated from the time-dependent ATR-IR spectra of the ruthenocene-initiated photopolymerization reaction of CA in the absence of any inhibitor. Solid lines indicate regions of positive correlation intensity; dashed lines indicate regions of negative correlation intensity. The one-dimensional spectrum shown on the top and side of the 2D plots is a representative spectrum taken from the data set used in the 2D analysis. (A) Autocorrelation within the 1700−1800 cm^{-1} spectral region. (B) Heterocorrelation between the 1700−1800 and 1150−1300 cm^{-1} spectral regions.

III.A. 2D IR Analysis of CA Photopolymerization. i. Asynchronous 2D IR Correlation. Asynchronous 2D IR correlation plots calculated from the ATR-IR spectra of the polymerization reaction in the absence of inhibitor are shown in Figure 7. In all the 2D IR and *kν* correlation plots presented here, positive peaks are represented by solid contour lines and negative peaks are represented by dashed contour lines. The signs of the asynchronous peaks indicate whether the intensity change at a particular frequency leads or lags when compared to other frequencies. The asynchronous map in Figure 7A shows the correlation of the spectral region between 1700 and 1800 cm^{-1} which contain the carbonyl stretching bands of the monomeric and the polymeric cyanoacrylate. A negative asynchronous doublet peak is observed between 1734 and 1754 cm^{-1}, which is a manifestation of the asynchronous relationship between the intensity changes of the two carbonyl bands. We have previously showed that an asynchronous cross-peak doublet is characteristic of two overlapped bands where the underlying subbands are changing intensity.[9] Figure 7B shows the asynchronous correlation between the regions 1700−1800 and 1150−1300 cm^{-1}. The latter region comprises the bands due to the ester C═O stretching and the ester C−O stretching vibrations. Positive cross-peaks are observed between 1754 vs 1285 cm^{-1} and 1754 vs 1188 cm^{-1}, while a negative cross-peak is observed between 1734 and 1250 cm^{-1}. Of note is the absence of an asynchronous cross-peak between the band at 1754 cm^{-1} (due to the carbonyl stretch of the saturated polymeric CA) and the band at 1250 cm^{-1} (due to the C−O ester stretch of the saturated polymeric CA); this implies that the intensity changes of these modes proceed at a similar rate. Also, the absence of pronounced asynchronous cross-peaks between the band at 1734 cm^{-1} (due to the carbonyl stretch of the conjugated monomeric CA) and the bands at 1190 and 1290 cm^{-1} (due to the C−O ester stretching vibrations of the conjugated monomeric CA) also implies that the intensity changes of these modes proceed at similar rates.

ii. kν Correlation Analysis. The *kν* correlation plots calculated from the ATR-IR spectra of the CA polymerization reaction in the absence of inhibitor are shown in Figure 8. The *kν* correlation map of the spectral region between 1700 and 1800 cm^{-1} is displayed in Figure 8A. A positive peak is seen at 1754 cm^{-1} with a k_{eff}^{+} value of 0.656. Negative peaks occur at 1754 and 1734 cm^{-1} with k_{eff}^{-} values of 0.05 and 0.55, respectively. The small negative peak at 1754 cm^{-1} appears since the rate of increase in intensity of this band decreases toward the end of the time interval chosen for the correlation. Figure 8B shows the *kν* correlation plot of the spectral region 1150−1300 cm^{-1}: a positive peak at 1250 cm^{-1} with a k_{eff}^{+} value of 0.68 and negative peaks at 1190, 1250, and 1290 cm^{-1} with k_{eff}^{-} values of 0.51, 0.05, and 0.53, respectively. The bands that are characteristic of the polymeric cyanoacrylate molecule (1754

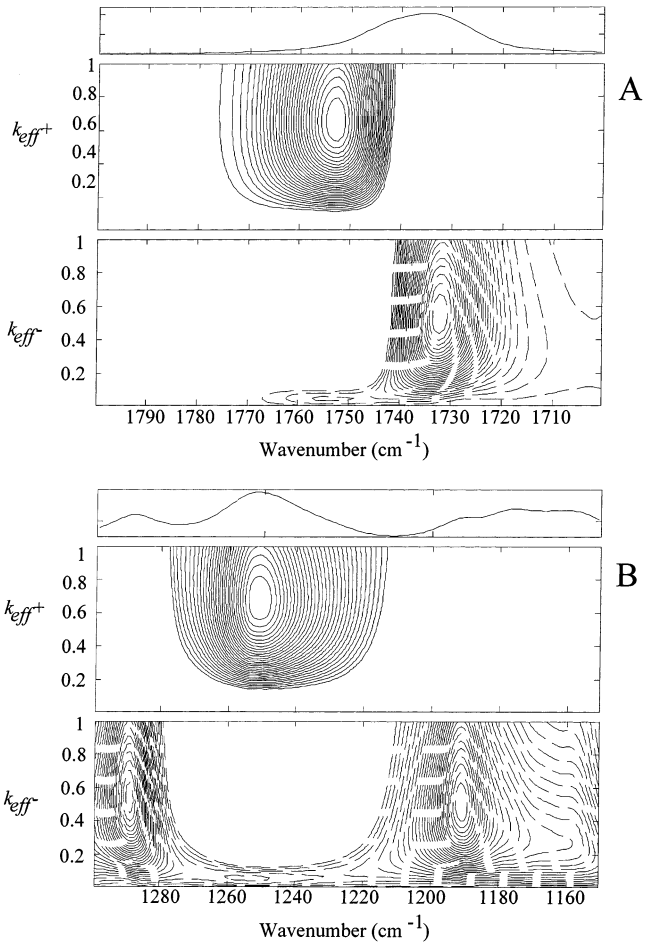

Figure 8. *kν* correlation plots calculated from the time-dependent ATR-IR spectra of the ruthenocene-initiated photopolymerization reaction of CA in the absence of any inhibitor. Solid lines indicate regions of positive correlation intensity; dashed lines indicate regions of negative correlation intensity. The one-dimensional spectrum shown on the top is a representative spectrum taken from the data set used in the *kν* analysis. Within each *kν* correlation plot, the top half indicates positive exponential correlation values (k_{eff}^+) while the bottom half indicates negative exponential correlation values (k_{eff}^-). (A) *kν* correlation plot in the region 1700−1800 cm^{-1}. (B) *kν* correlation plot in the region 1150−1300 cm^{-1}.

TABLE 5: Values of the Effective Rate Constants k_{eff}^+ and k_{eff}^-, Obtained from the *kν* Correlation Plot in Figure 8[a]

wavenumber (cm^{-1})	band assign	k_{eff}^+	k_{eff}^-
1753	polymeric ester C═O	0.66	0.05
1732	monomeric ester C═O	−	0.55
1616	monomeric C═C	−	0.48
1251	polymeric ester C−O	0.68	0.05
1290	monomeric ester C−O	−	0.53
1190	monomeric ester C−O	−	0.51

[a] These effective rate constants were obtained from the time-dependent ATR-IR spectra of the $RuCp_2$ photoinitiated polymerization of CA in the absence of an inhibitor.

and 1251 cm^{-1}) have very similar k_{eff}^+ and k_{eff}^- values, as seen in Table 5, implying that the ongoing polymerization reaction affects these bands simultaneously. This is logical, since both bands arise from the carbonyl ester group in the saturated polymeric cyanoacrylate molecule. The bands characteristic of the monomeric CA at 1190, 1290, and 1734 cm^{-1} have negative bands with similar k_{eff}^- values indicating similar decreasing rates of intensity change. A comparison of the absolute k_{eff} values

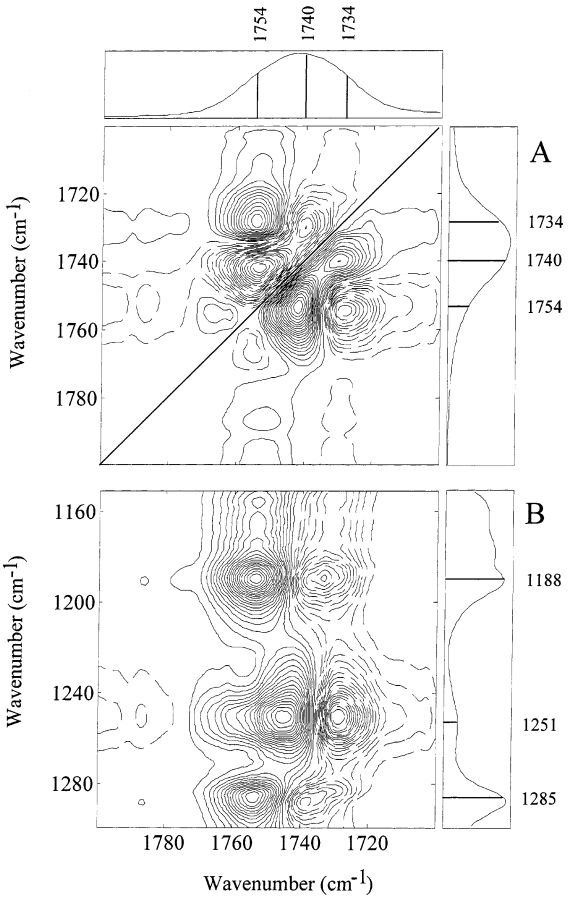

Figure 9. Asynchronous 2D IR correlation plots calculated from the time-dependent ATR-IR spectra of the ruthenocene-initiated photopolymerization reaction of CA in the presence of the inhibitor MSA. Solid lines indicate regions of positive correlation intensity; dashed lines indicate regions of negative correlation intensity. The one-dimensional spectrum shown on the top and side of the 2D plots is a representative spectrum taken from the data set used in the 2D analysis. (A) Autocorrelation within the 1700−1800 cm^{-1} spectral region. (B) Heterocorrelation between the 1700−1800 and 1150−1300 cm^{-1} spectral regions.

for the monomeric and polymeric vibrational modes indicates that polymeric bands both have k_{eff}^+ values (∼0.66−0.68) that are larger than the k_{eff}^- values of the monomeric modes (∼0.48−0.55). This difference indicates the increase in intensity of the saturated polymeric CA begins earlier than the decrease in intensity of the bands due to the conjugated monomeric CA, and that the polymerization reaction is slightly out-of-phase with depletion of the monomer.

III.B. 2D IR Analysis of CA Photopolymerization in the Presence of Inhibitor. i. Asynchronous 2D IR Correlation. Asynchronous 2D IR correlation plots calculated from the ATR-IR spectra of the polymerization reaction in the presence of the reaction inhibitor methane sulfonic acid (MSA) are shown in Figure 9. The region between 1700 and 1800 cm^{-1} that is indicative of the carbonyl stretching bands of the monomeric and the polymeric cyanoacrylate is shown in Figure 9A. There are significant differences between the 2D IR correlation maps of CA in the presence of the MSA inhibitor (Figure 9A) and in the absence of the inhibitor (Figure 7A). Positive cross-peaks are observed at 1742 vs 1754 cm^{-1} and 1730 vs 1754 cm^{-1} in the asynchronous map (Figure 9A). In addition, a negative asynchronous peak is now observed at 1730 vs 1740 cm^{-1}, resulting in an elongated quartet of cross-peaks. We have previously showed that an elongated asynchronous cross-peak quartet is characteristic of a single band undergoing a frequency

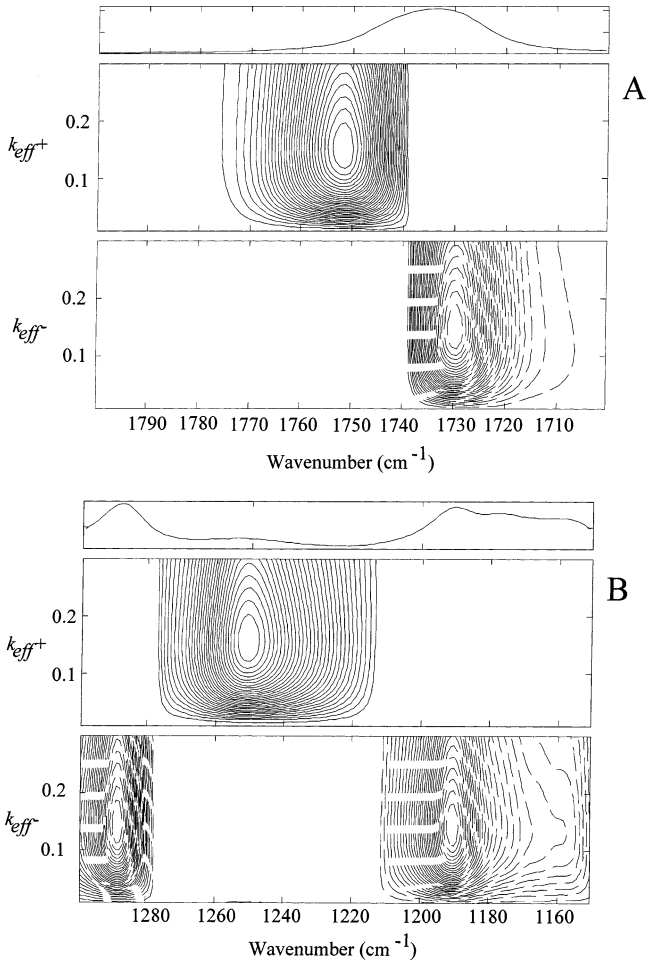

Figure 10. *kν* correlation plots calculated from the time-dependent ATR-IR spectra of the ruthenocene-initiated photopolymerization reaction of CA in the presence of the MSA inhibitor. Solid lines indicate regions of positive correlation intensity; dashed lines indicate regions of negative correlation intensity. The one-dimensional spectrum shown on the top is a representative spectrum taken from the data set used in the *kν* analysis. Within each *kν* correlation plot, the top half indicates positive exponential correlation values (k_{eff}^+) while the bottom half indicates negative exponential correlation values (k_{eff}^-). (A) *kν* correlation plot in the region 1700−1800 cm^{-1}. (B) *kν* correlation plot in the region 1150−1300 cm^{-1}.

shift.[9] Therefore, the presence of the MSA inhibitor appears to change the underlying polymerization mechanism as it affects the C═O band. Figure 9B shows the asynchronous correlation plot between the 1700−1800 cm^{-1} and the 1150−1300 cm^{-1} regions. In this plot, cross-peaks are observed between vibrational modes attributable to the CA polymer and monomer, e.g. positive cross-peaks at 1754 vs 1285 cm^{-1} and 1754 vs 1188 cm^{-1}, and negative cross-peaks at 1730 vs 1251 cm^{-1} and 1733 vs 1190 cm^{-1}. The presence of asynchronicity between polymer and monomer modes indicates the mutually independent reorientation of the two types of CA molecules during the polymerization reaction.

ii. kν Correlation Analysis. The *kν* correlation plots of the ATR-IR spectra of the ruthenocene-mediated polymerization reaction in the presence of the MSA inhibitor are displayed in Figure 10. The *kν* correlation map of the C═O spectral region between 1700 and 1800 cm^{-1} is displayed in Figure 10A. A positive *kν* correlation peak is seen at 1754 cm^{-1} with a k_{eff}^+ value of 0.15 while a negative peak is observed at 1734 cm^{-1} with a k_{eff}^- value of 0.15. Figure 10B shows the *kν* correlation plot of the spectral region 1150−1300 cm^{-1} where a positive peak at 1251 cm^{-1} ($k_{eff}^+ = 0.16$) and negative peaks at 1190 c ($k_{eff}^- = 0.14$) and 1290 cm^{-1} ($k_{eff}^- = 0.15$) are observed. A comparison of the absolute k_{eff} values for the monomeric and polymeric vibrational modes in Table 6 indicates that both polymeric modes have k_{eff}^+ values (∼0.15−0.16) that are virtually the same as the k_{eff}^- values of the monomeric modes (∼0.14−0.15). This indicates the increase in intensity of the saturated polymeric CA begins in concert with the decrease in intensity of the bands due to the conjugated monomeric CA and that the polymerization reaction is in-phase with depletion of the monomer. This differs from the case of CA polymerization in the absence of additional MSA inhibitor (Figure 8 and Table 5). The *kν* correlation method was thus able to show how the polymerization behavior of CA in the presence of inhibitor differed from that of CA in the absence of inhibitor.

TABLE 6: Values of the Effective Rate Constants k_{eff}^+ and k_{eff}^-, Obtained from the *kν* Correlation Plot in Figure 10[a]

wavenumber (cm^{-1})	band assign	k_{eff}^+	k_{eff}^-
1753	polymeric ester C═O	0.15	−
1732	monomeric ester C═O	-	0.15
1616	monomeric C═C	−	0.14
1251	polymeric ester C−O	0.16	−
1290	monomeric ester C−O	−	0.15
1190	monomeric ester C−O	−	0.14

[a] These effective rate constants were obtained from the time-dependent ATR-IR spectra of the $RuCp_2$ photoinitiated polymerization of CA in the presence of MSA as an inhibitor.

Conclusions

Our laboratory has previously developed an approach called *βν* correlation analysis to quantitatively describe the degree of coherence between spectral intensity changes and the sequence of molecular events in a set of dynamic spectra.[15] This method utilizes defined mathematical models as complementary functions to experimental data sets in the correlation algorithm. In the work described in this article, we have expanded the scope of this method to encompass exponential relationships between spectral intensities using a technique called *kν* correlation analysis.

A *kν* correlation analysis is a mathematical asynchronous cross correlation performed between a set of *N* spectra undergoing some dynamic intensity variation against a set of exponential functions with a user-defined range of rate constants. As such, it is a model-dependent 2D IR correlation method analogous to the *βν* method previously described. In *kν* correlation analysis, the observed correlation intensities are a function of the rate constant of the exponential function and the spectral frequency. The 2D correlation plots reveal rate relationships between different molecular events in terms of a quantitative and tangible parameter, *k*, which is the rate constant of the exponential function used in the correlation. A new parameter, the effective rate constant, k_{eff}, is defined as the point of maximum correlation intensity at particular frequencies in the plot of *k* vs *ν*. The calculated values of k_{eff} represent the rates at which the intensities of the spectral bands change during the course of the dynamic experiment. As a result, these k_{eff} values are comparable and can be used to assign quantitative rate relationships. Events at frequencies with a larger k_{eff} value occur earlier than events at frequencies with smaller k_{eff} values. Positive and negative k_{eff} values are comparable and hence no manipulation of the spectra or the correlation plots is required to compare bands with increasing and decreasing intensities.

Using simulated IR spectra, we applied *kν* correlation analysis to several intensity variation models. On the basis of these

results, we showed that *kν* correlation methods are sensitive to the *relative change* in the rates of the band intensities through the dynamic data set. The k_{eff} values are not the actual kinetic rate constants per se, but are instead the *relative differences* of the rates defined by the rate constants used in the correlation calculation. The k_{eff} parameter is sensitive to the *relative order* in which the intensity change occurs, while the size of the correlation peaks gives an indication of the *magnitude* of the intensity change. Spectral bands whose rate of intensity change varies through a dynamic data set are distinguished by the presence of both positive and negative peaks in the *kν* correlation plots.

We applied the *kν* correlation analysis method to the photoinitiated polymerization reaction of 2-ethyl-cyanoacrylate. ATR-IR spectra of the anionic polymerization reaction of CA with ruthenocene as a photoinitiator were collected both in the presence and in absence of an inhibitor (methane sulfonic acid). The resulting time-dependent IR spectra were analyzed by using the *kν* correlation method. Analysis of the k_{eff} effective rate constants showed that, in the absence of the inhibitor, the vibrational modes corresponding to the polymeric CA molecule show reaction earlier in the polymerization process than do the vibrational modes attributable to the monomeric CA molecule. When an inhibitor is present, both monomer and polymer modes undergo intensity changes at approximately the same rate.

Acknowledgment. The work described here was supported by the U.S. Public Health Service through National Institutes of Health grant EB001956 (R.A.D.).

References and Notes

(1) Noda, I. *Appl. Spectrosc.* **1990**, *44*, 550.
(2) Noda, I. *Appl. Spectrosc.* **1993**, *47*, 1329.
(3) Harrington, P. d. B.; Urbas, A.; Tandler, P. J. *Chemom. Intell. Lab. Syst.* **2000**, *50*, 149.
(4) *Two-Dimensional Correlation Spectroscopy*; Ozaki, Y., Noda, I., Eds.; American Institute of Physics: New York, 2000.
(5) Noda, I.; Story, G. M.; Marcott, C. *Vib. Spectrosc.* **1999**, *19*, 461.
(6) Filosa, A.; Wang, Y.; Ismail, A. A.; English, A. M. *Biochemistry* **2001**, *40*, 8256.
(7) Paquet, M.-J.; Laviolette, M.; Pezolet, M.; Auger, M. *Biophys. J.* **2001**, *81*, 305.
(8) Graff, D. K.; Pastrana-Rios, B.; Venyaminov, S. Y.; Prendergast, F. G. *J. Am. Chem. Soc.* **1997**, *119*, 11282.
(9) Elmore, D. L.; Dluhy, R. A. *Colloids Surf. A* **2000**, *171*, 225.
(10) Elmore, D. L.; Dluhy, R. A. *Appl. Spectrosc.* **2000**, *54*, 956.
(11) Elmore, D. L.; Shanmukh, S.; Dluhy, R. A. *J. Phys. Chem. A* **2002**, *106*, 3420.
(12) Shanmukh, S.; Howell, P.; Baatz, J. E.; Dluhy, R. A. *Biophys. J.* **2002**, *83*, 2126.
(13) Pancoska, P.; Kubelka, J.; Keiderling, T. A. *Appl. Spectrosc.* **1999**, *53*, 655.
(14) Kubelka, J.; Pancoska, P.; Keiderling, T. A. *Appl. Spectrosc.* **1999**, *53*, 666.
(15) Elmore, D. L.; Dluhy, R. A. *J. Phys. Chem. B* **2001**, *105*, 11377.
(16) Noda, I. *Appl. Spectrosc.* **2000**, *54*, 994.
(17) Eads, C. D.; Noda, I. *J. Am. Chem. Soc.* **2002**, *124*, 1111.
(18) Geoffroy, G. L.; Wrighton, M. S. *Organometallic Photochemistry*; Academic Press: New York, 1979.
(19) Akiyama, T.; Hoshi, Y.; Goto, S.; Sugimori, A. *Bull. Chem. Soc. Jpn.* **1973**, *46*, 1851.
(20) Borrell, P.; Henderson, E. *J. Chem. Soc., Dalton* **1975**, *5*, 432.
(21) Grandbois, M.; Desbat, B.; Blaudez, D.; Salesse, C. *Langmuir* **1999**, *15*, 6594.
(22) Bergamini, P.; Dimartino, S.; Maldotti, A.; Sostero, S.; Traverso, O. *J. Organomet. Chem.* **1989**, *365*, 341.
(23) Sanderson, C. T.; Palmer, B. J.; Morgan, A.; Murphy, M.; Dluhy, R. A.; Mize, T.; Amster, I. J.; Kutal, C. *Macromolecules* **2002**, *35*, 9648.
(24) Lin-Vien, D.; Colthup, N. B.; Fateley, W. G.; Grasselli, J. G. *The Handbook of Infrared and Raman Characteristic Frequencies of Organic Molecules*; Academic Press: San Diego, CA, 1991.